

MultiGraspNet: A Multitask 3D Vision Model for Multi-gripper Robotic Grasping

Stephany Ortuno-Chanelo¹, Paolo Rabino¹, Enrico Civitelli², Tatiana Tommasi¹, Raffaello Camoriano^{1,3}

Abstract—Vision-based models for robotic grasping automate critical, repetitive, and draining industrial tasks. Existing approaches are typically limited in two ways: they either target a single gripper and are potentially applied on costly dual-arm setups, or rely on custom hybrid grippers that require ad-hoc learning procedures with logic that cannot be transferred across tasks, restricting their general applicability. In this work, we present *MultiGraspNet*, a novel multitask 3D deep learning method that predicts feasible poses simultaneously for parallel and vacuum grippers within a unified framework, enabling a single robot to handle multiple end-effectors. The model is trained on the richly annotated GraspNet-1Billion and SuctionNet-1Billion datasets, which have been aligned for the purpose, and generates graspability masks quantifying the suitability of each scene point for successful grasps. By sharing early-stage features while maintaining gripper-specific refiners, *MultiGraspNet* effectively leverages complementary information across grasping modalities, enhancing robustness and adaptability in cluttered scenes.

We characterize *MultiGraspNet*’s performance with an extensive experimental analysis, demonstrating its competitiveness with single-task models on relevant benchmarks. We run real-world experiments on a single-arm multi-gripper robotic setup showing that our approach outperforms the vacuum baseline, grasping 16% more seen objects and 32% more of the novel ones, while obtaining competitive results for the parallel task.

Index Terms—Robotic grasping, Multi-gripper grasping, 3D Perception, Multitask Learning

I. INTRODUCTION

IN recent years, the demand for robotic systems in industrial and warehouse environments has grown significantly, expanding toward increasingly diverse and complex tasks. This trend is driven by the need to improve operational efficiency and working conditions, while reducing safety risks for human operators. A central challenge in this context is the development of robotic systems capable of handling a wide variety of items that differ in shape, size, weight, and material properties. In response, research in autonomous grasping has led to increasingly sophisticated solutions that integrate computer vision, machine learning, and robotics to perceive, localize, and manipulate objects in cluttered environments.

Classical robotic grasping systems employ a single gripper, most commonly either a parallel gripper or a vacuum gripper. The former relies on frictional contacts and is best suited to rigid objects that provide sufficient friction and stable contact geometry for force closure [1], [2]. The latter is most effective for objects with smooth, low-porosity surfaces that

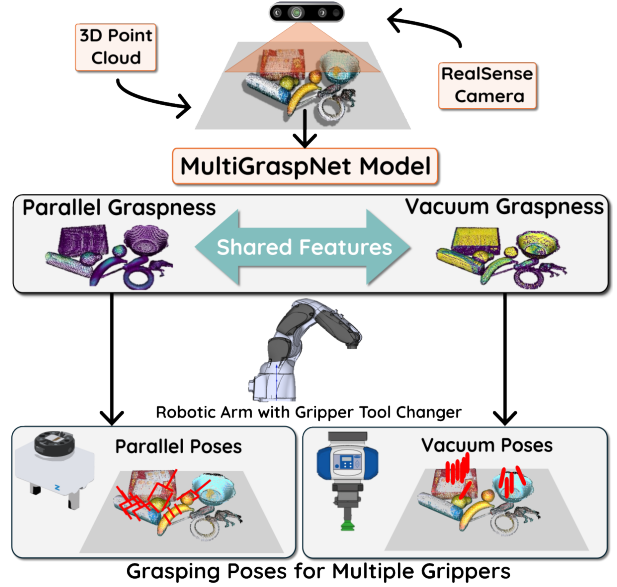


Fig. 1: Overview of MultiGraspNet. Our proposed multi-gripper approach is formulated as a multitask deep network that processes a 3D scene point cloud and learns a shared representation to jointly predict grasping quality scores for parallel and vacuum grippers based on geometric cues. The resulting graspness maps identify graspable regions in cluttered scenes and are further refined to produce the final grasp poses for both the parallel and suction grippers.

can form a seal [3]–[5]. Although using one end-effector is cost-effective and simplifies grasp planning, performance is limited by the mechanical and geometric properties of the selected gripper. Thus, single-gripper robots often struggle to reliably grasp a diverse range of objects, reducing their adaptability and effectiveness. These limitations have been addressed through the development of custom hybrid grippers combining suction cups [6], compliant fingers [7], or sensor-integrated fingertips [8], [9]. Such grippers are typically tailored to specific object characteristics, achieving high performance in targeted applications, but exhibiting limited adaptability when confronted with novel items or unanticipated configurations, which hinders generalization.

Recently designed systems overcome these issues by using different grippers with multiple robotic arms, working collaboratively to handle a broader range of objects [10], [11]. However, they present increased spatial requirements, financial costs, and overall complexity. Furthermore, despite improving grasping capabilities, these systems typically rely on separate, gripper-specific grasp prediction models, which can lead to

¹VANDAL Laboratory, Department of Control and Computer Engineering, Politecnico di Torino, Turin, Italy.

²Comau S.p.A., Advanced Automation Solutions, Grugliasco, Italy.

³Istituto Italiano di Tecnologia, Genoa, Italy.

suboptimal learning. Because each model is trained independently, the learned representations are separate, preventing positive knowledge transfer and ultimately limiting generalization to unseen objects and scenarios. In this context, multi-gripper methods for a single robotic arm represent an underexplored, yet promising direction that can strike the balance between cost and performance. Crucially, the challenge goes beyond designing and controlling a robot capable of switching among multiple end-effectors, and calls for learning a multi-objective shared model within a single framework. Such a model should build a unified internal representation that supports multiple grasping tasks and enables effective information transfer across grasping modalities.

For this purpose, we introduce our *MultiGraspNet*, a novel 3D vision-based multitask deep learning architecture that predicts grasping poses for multiple grippers simultaneously. Overcoming the need for multiple specialized models, MultiGraspNet leverages both early-stage shared representations and specialized pose refiners to extract tailored features for each gripper while transferring knowledge across tasks, resulting in improved grasping success rate and a unified learning pipeline. Our approach, outlined in Fig. 1, allows a single robotic arm to utilize two distinct grippers: a parallel-jaw gripper and a vacuum gripper. This configuration enhances the versatility of the robot, allowing it to handle a significantly broader range of objects while reducing hardware and computational costs.

To summarize, our main contributions are:

- We introduce MultiGraspNet, a multitask 3D deep learning model capable of generating multiple candidate poses for vacuum and parallel grippers simultaneously from 3D visual input of cluttered scenes.
- We evaluate our system with an extensive experimental analysis including benchmark comparisons, design-choice and data-regime analyses, and real-world grasping experiments on known and novel objects in an industrial scenario.

Our results demonstrate MultiGraspNet’s advantage over single-task baselines and highlight the potential of multitask learning for scalable and robust multi-gripper robotic manipulation, paving the way for future research on unified grasping models and more adaptive robotic systems.

II. RELATED WORKS

A. Suction Grasping

Suction-based grasping is a particularly effective solution in cluttered environments due to its simplicity. Early approaches to suction grasp prediction primarily relied on convolutional neural networks (CNNs) to infer grasp poses from RGB or depth images, while alternative methods exploited purely geometric reasoning on point clouds: [12] proposed a hybrid ResNet-based U-Net architecture for dense suction grasp prediction without requiring explicit object recognition. SuctionNet-1Billion (S1B) [13] further advanced the field through a two-stage framework that integrates physics-based grasp evaluation and provides a large-scale benchmark for online evaluation.

Concerning 3D perception-based approaches, the Grasp Quality CNN (GQ-CNN) [3] method trained on the synthetic

Dex-Net 3.0 dataset demonstrated strong generalization capabilities on novel objects. More recently, SGNet [14] showed how to predict suction grasp parameters and object centers directly from point cloud data, while UISN [4] proposed a multi-stage pipeline that focuses on unseen objects by using Unseen Object Instance Segmentation (UOIS) [15] and includes the estimation of instance-level suction scores with associated uncertainty.

Despite their effectiveness, these methods tend to perform best on relatively regular and flat objects, while being less reliable on highly textured or deformable objects, and on surfaces that hinder the formation of an airtight suction seal.

B. Parallel Grasping

Early approaches for parallel grasp detection from visual input introduced the grasping rectangle representation [16]. Building on this idea, [17] proposed a cascaded two-network system that prunes unlikely grasps to balance speed and robustness. Subsequent works introduced region-based detectors combining global and local candidates to improve robustness and precision [18]. More recently, RGBD-Grasp [19] decomposed parallel grasp prediction into two sub-tasks: inferring position and orientation, followed by grasp width and depth.

Among 3D perception-based methods, Dex-Net 2.0 [1] introduced a large-scale synthetic set of point clouds and grasping poses, with a first version of the GQ-CNN model that predicted parallel grasp success probabilities. Recognizing the need for larger datasets and better evaluation systems, GraspNet-1Billion [20] provided a massive data collection from the real world with annotations obtained by analytic computation in simulation. To improve grasp candidate selection, GSNet [21] introduced the concept of *graspness*, a geometry-driven quality measure, and developed a fast end-to-end network integrating it. The authors of [22] introduced an end-to-end deep learning approach leveraging differentiable sampling. More recently, EconomicGrasp (EFG) [2] tackled the challenge of costly supervision by efficiently selecting labels with low ambiguity. GenGrasp [23], instead, explicitly modeled grasping physical priors to enhance novel object manipulation.

Although parallel-gripper approaches are well-suited for handling complex objects, they can face difficulties with large or flat objects of limited height. In such cases, incorporating an end-effector with complementary capabilities, such as a vacuum gripper, can enhance effectiveness.

C. Multi-gripper Grasping

To overcome the limitations of each end-effector, several studies focused on the adoption of multi-functional grippers. For instance, Carman [24] won the Amazon Robotics Challenge in 2017 with a custom grasping tool that included suction and parallel grippers. Their model relied on a semantic segmentation network to predict grasping poses, followed by heuristic grasp synthesis. In the same challenge, [6] presented an approach for predicting affordance maps over four grasping primitives, enabling the use of a custom gripper that combines suction and parallel grasping. Instead, [10] proposed a robot system able to use two gripper combinations via a switching strategy. It exploited a Single Shot MultiBox Detector (SSD) network that

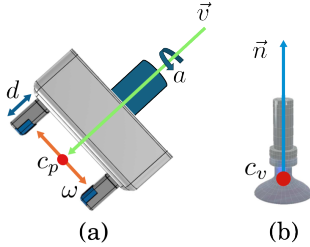


Fig. 2: Schematic illustration of the parallel-jaw gripper (a) and vacuum gripper (b) poses. The former includes the central point c_p , the depth d , the width ω , as well as the approach direction v and angle a . The vacuum grasp pose includes the central point c_v and the normal to the point n .

includes objectness prediction, and the choice of the gripper is based on the sparseness of the identified object items. In [11], a switching strategy was introduced for suction and multi-fingered grippers to perform random bin picking and assembly applications. Even in this case the learning component was limited to object recognition and localization.

Dex-Net 4.0 [25] trained separate GQ-CNNs to predict the probability of grasp success for parallel and suction grippers given a point cloud, rather than pursuing a unified model. In contrast, Corner-Grasp [26] introduced a multitask learning approach that infers 2D grasping poses for multiple grippers and predicts surface material to select the grasping modality.

While prior work on multi-gripper grasping began exploring the benefits of multitask learning for jointly modeling multiple grasping modalities, existing approaches are primarily validated on 2D data in synthetic environments or are constrained by custom hardware. Building on this emerging direction, our MultiGraspNet introduces a multitask framework that operates in 3D on real-world data, enabling knowledge transfer across related grasping strategies to improve grasping robustness.

III. METHOD

A. Task Definition

We introduce a unified multitask deep learning framework that enables a single model to predict grasping poses for heterogeneous end-effectors, namely parallel and vacuum grippers, as illustrated in Fig. 2. Our approach is designed to increase the system’s versatility by leveraging the advantages of each gripper while transferring knowledge between tasks.

Given an input scene $\{p_i \in \mathbb{R}^3\}_{i=1}^N$, formally represented as a 3D point cloud of size N , the goal of our model is to predict candidate grasping poses for two gripper types simultaneously. Following the conventions established in [2], we define the 3D grasping pose for the parallel-jaw gripper as:

$$G_p = [c_p, v, a, \omega, d, s_p], \quad (1)$$

where c_p indicates the central point of the grasp in the 3D space, v is the approaching direction vector and a [$^\circ$] represents the angle of the 2D in-plane rotation. The remaining three components d , ω , and s_p are respectively the depth [m], which is the distance from the grasp point to the origin of the gripper frame, the width [m], that describes the distance between the

fingers needed to grasp the object, and the grasp score which indicates the quality of the pose.

For the vacuum-based gripper, the grasp pose is represented as in [13]:

$$G_v = [c_v, n, s_v], \quad (2)$$

where c_v is the central grasp point in the 3D space, n is an estimate of the 3D surface normal vector in that point, and s_v is the vacuum score indicating the quality of the pose.

B. Dataset with Multi-gripper Graspness Map

To meet this requirement, we propose to integrate the GraspNet-1Billion [20] and SuctionNet-1Billion [12] datasets, which share a common set of objects and scenes. By aligning their grasp annotations, it is possible to build a unified label space. Specifically, a *graspness score map* that encodes the suitability of different regions in the scene for successful grasping across multiple end-effectors is defined. This design enables multitask training while allowing direct and fair comparisons with single-task methods.

For the parallel gripper, the map is computed by starting from the provided friction coefficient and using the look-ahead search strategy for grasp success introduced in [21], and already adopted in [2]. In this letter this strategy is extended to the vacuum task over single 3D object models by considering the provided seal coefficient and filtering out unsuccessful grasps (coefficient below 0.004). Then, the graspness map is obtained at the scene level by using the 6D pose for each object and filtering out the poses with collisions. Finally, the map is projected onto the original point cloud.

To exclude non-graspable locations, points outside the operational zone (table depth < 0) are pruned, and background points not belonging to any object instance using the *objectness* score o . Then, a nearest neighbor search associates each point in the scene with the closest grasp point and its properties. This process ensures that our graspness map is defined directly over the scene’s geometry, allowing it to be visualized and employed as training data. The per-point vacuum graspness map is rescaled to the $[0, 1]$ range, after which low-quality grasp regions are filtered out (scores below 0.1).

Overall, a supervised multi-gripper graspness map with the needed s_p and s_v values is constructed, derived from physically accurate grasping poses and accounting for the force-closure coefficient in the case of the parallel gripper and the seal coefficient for the vacuum gripper. This formulation enables the model to learn meaningful graspability patterns grounded in physically valid grasp configurations.

C. MultiGraspNet

Our newly designed multi-gripper model is presented in Fig. 3. The rest of this section describes its main components.

1) *Backbone Network*: Similar to previous approaches [2], [21], we use a 3D U-Net as the main backbone, which is based on MinkowskiEngine [27]. The backbone encodes geometric scene information into per-point vectors, providing as output a feature tensor of shape $[N, 512]$.

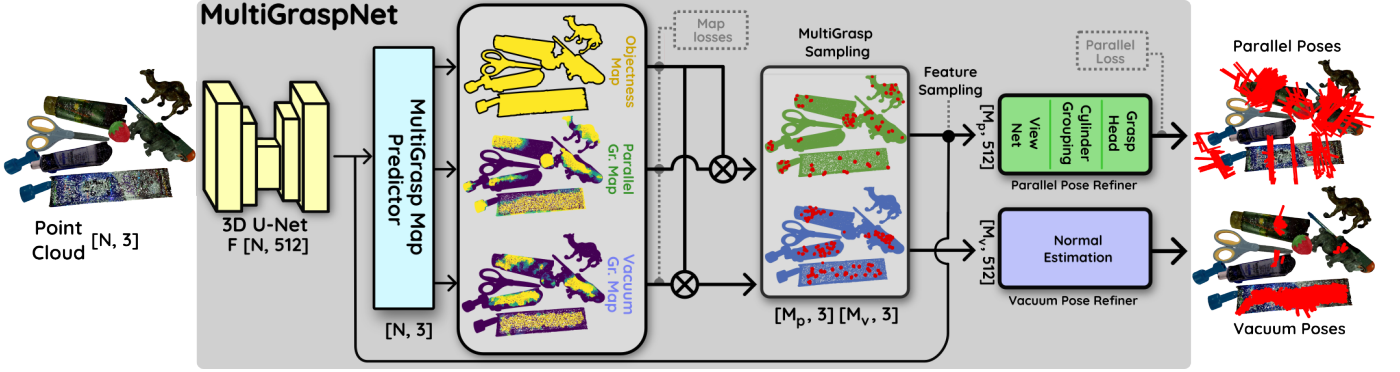


Fig. 3: Overview of our architecture. The network takes as input a 3D point cloud. Then the Minkowski-based backbone extracts geometric features. The features are then processed by a multi-branch grasp prediction head to predict the objectness and the graspsness masks for each gripper. Finally, gripper-specific refinement modules are applied to generate the multi-gripper grasping poses.

2) *MultiGrasp Map Predictor*: This module consists of three heads that elaborate in parallel on the features to output, respectively, the objectness score \tilde{o} , the graspsness scores for the parallel gripper \tilde{s}_p , and the graspsness scores for the vacuum gripper \tilde{s}_v . Every head is defined by a 1D convolutional layer that independently predicts a score for each point, obtaining a $[N, 3]$ -dimensional output that can be visualized onto the scene as the graspsness and objectness maps. During training, the objectness head is optimized using a cross-entropy loss, while the vacuum graspsness head employs a binary cross-entropy loss. For the parallel graspsness head, we use a weighted binary cross-entropy, assigning a ten-fold higher weight to positive samples to address class imbalance. We emphasize that the graspsness score \tilde{s}_p is only an intermediate output, used to guide the network toward potentially graspable points, while the full parallel-grasp pose is predicted in later stages of the network.

3) *MultiGrasp Sampling*: Combining the task-specific graspsness maps with objectness enables the identification of object points with a high probability of successful grasping. We formalize this via per-point score pair multiplication (denoted by \otimes in Fig. 3), followed by thresholding (t_p and t_v) to discard low-scoring points. The points are further sub-selected using Farthest Point Sampling (FPS) to maximize spatial coverage. The resulting M_p , M_v seed points for the parallel and vacuum grippers, along with their 512-dimensional backbone features, are then fed into the corresponding pose refiner modules.

4) *Parallel Pose Refiner*: Concerning the parallel grasping task, we follow the process in [2] for each of the M_p points. The *ViewNet* module uses probabilistic view selection to determine approaching vectors \tilde{v} . Guided by these vectors, directional cylinders with fixed height and radius are used to group points to form grasp candidates within the so-called *Cylinder Grouping* process. Finally, these candidates are processed by a *Grasp Head* to produce the width $\tilde{\omega}$, the in-plane rotation $\tilde{\alpha}$, the depth \tilde{d} , as well as the graspsness score \tilde{s}_p . The training process optimizes a Smooth L1 loss for view and width prediction, while a cross-entropy loss is adopted for the in-plane angle and depth. As in [2], the graspsness score estimation is formulated as a classification task and supervised via a cross-entropy loss.

5) *Vacuum Pose Refiner*: The vacuum pose prediction follows a different strategy due to the simpler nature of the pose. The refiner does not need further losses and is only adopted at inference time. For each of the points in M_v , the surface normal vector \tilde{n} is estimated by looking at the geometry of its nearby neighbors. Using an off-the-shelf normal estimation method [28], a small radius is used to find the closest points around each seed, and the normal vector is computed by analyzing the local shape through covariance to fit the best local surface. These normals complete the vacuum poses directly from point geometry without requiring additional view selection or grouping operations. Overall, the design of our multi-gripper model combines the advantages of feature sharing and task-specific refiners to handle the unique characteristics of different end-effectors, enabling multi-grasp predictions within a single unified framework, avoiding the use of costly separate architectures.

D. Implementation Details

Our approach addresses two tasks corresponding to two end-effectors (vacuum and parallel). The parallel task is guided by the combination of the relative graspsness map and pose prediction losses, whereas the vacuum task relies solely on the loss of its vacuum graspsness map. To efficiently integrate these tasks, we adopt the Gradient Surgery for Multitask Learning (PCGrad) technique [29] during training, which mitigates conflicting gradient updates across tasks.

For training, we use the Adam optimizer with an initial learning rate of 5×10^{-4} and a cosine decay scheduler. The batch size is set to 12, and training runs for 22 epochs. Regarding the internal parameters of our model, we define the number of seeds M_p and M_v equal to 1024 and the threshold to discard low-scoring points for each gripper t_a and t_v as 0.1. All experiments are conducted using PyTorch on a single NVIDIA GeForce RTX 5090 GPU.

IV. EXPERIMENTS

A. Experimental Protocol and Metrics

The defined dual-gripper dataset comprises 190 scenes, of which 100 are used for training and 90 for testing. Follow-

TABLE I: Single-task results on the RealSense data of the aligned dual-gripper dataset from SuctionNet-1Billion (Vacuum) and GraspNet-1Billion (Parallel). Top results are in bold, while the second best are underlined.

Method	Vacuum								
	Seen			Similar			Novel		
	AP	AP _{0.8}	AP _{0.4}	AP	AP _{0.8}	AP _{0.4}	AP	AP _{0.8}	AP _{0.4}
DexNet3.0 [3]	15.50	1.53	20.22	18.92	2.62	24.51	2.62	0.35	5.32
S1B [13]	28.31	3.41	38.56	26.64	3.42	35.34	8.23	0.35	10.29
MultiGraspNet-vac.	28.26	<u>3.60</u>	<u>36.39</u>	31.37	3.88	41.63	<u>8.07</u>	0.48	<u>10.03</u>
MultiGraspNet	28.07	3.62	35.81	<u>31.22</u>	<u>3.53</u>	41.65	7.38	<u>0.46</u>	8.92

Method	Parallel								
	Seen			Similar			Novel		
	AP	AP _{0.8}	AP _{0.4}	AP	AP _{0.8}	AP _{0.4}	AP	AP _{0.8}	AP _{0.4}
G1B [20]	27.56	33.43	16.95	26.11	34.18	14.23	10.55	11.25	3.98
GSNet [21]	67.12	78.46	60.90	54.81	66.72	46.17	24.31	30.52	14.32
EFG [2]	68.21	<u>79.60</u>	<u>63.54</u>	61.19	73.60	<u>53.77</u>	<u>25.48</u>	<u>31.46</u>	<u>13.85</u>
MultiGraspNet-par.	67.70	78.97	62.67	<u>60.61</u>	72.51	54.01	25.45	31.36	13.60
MultiGraspNet	68.37	79.61	64.02	60.28	<u>72.54</u>	52.87	25.53	31.67	13.66

ing [13], [20], we divide the test set into three groups of equal size: seen/similar/novel. This enables us to evaluate how different methods generalize in increasingly complex scenarios. The grasp prediction modules generate multiple grasp candidates for each scene. Therefore, by following standard practice [13], [20], we adopt Precision@ k as our evaluation metric, which measures precision among the top- k ranked grasps. We denote by AP_{μ_p} and AP_{μ_v} the Average Precision@ k for the parallel and vacuum tasks respectively, with k ranging from 1 to 50. The subscripts μ_p and μ_v refer to specific friction (parallel) and seal (vacuum) coefficients. Note that a high μ_p indicates that the gripper applies a large force, which generally leads to a higher-quality grasp. For the vacuum gripper, a grasp is considered positive only when the seal coefficient exceeds the value indicated by the subscript. Therefore, a high μ_v corresponds to a more selective and stricter success criterion. We also report the overall AP as the average result with μ_p ranging from 0.2 to 1.0 and μ_v ranging from 0.2 to 0.8, both with an interval of 0.2.

B. Benchmark Comparison

We compare the results of our MultiGraspNet with well-established single-gripper approaches, including S1B [13], DexNet3.0 [3] for the vacuum, and G1B [20], GSNet [18], EFG [2] for the parallel end-effector. For a comprehensive and fair benchmark, we also report the performance of single-task variants of our approach, either vacuum or parallel, obtained by deactivating the objective of the other gripper during training while preserving the full network architecture.

Table I reports the evaluation results for the RealSense camera, clearly indicating that novel objects are more challenging to grasp than seen or similar ones. More precisely, the upper section of the table presents the vacuum grasping results. For $AP_{0.8}$, our vacuum-specific variant *MultiGraspNet-vac.* consistently outperforms competing methods across all object groups. This advantage is particularly pronounced for similar objects, where improvements are also observed for $AP_{0.4}$ and AP . The full multitask version MultiGraspNet

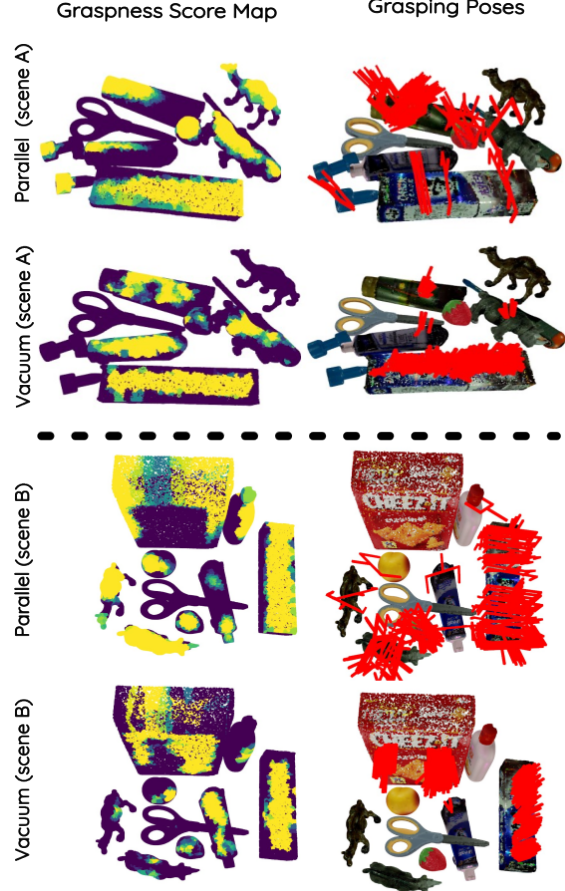


Fig. 4: Qualitative results of MultiGraspNet. For each scene, our model predicts a graspness score map and poses for the vacuum and parallel grippers. We show the top 100 grasps, ranked by the predicted grasp scores for each gripper.

preserves the gain in most of the considered cases, with minor positive or negative fluctuations. We remark that the baselines operate on 2D image inputs and are substantially larger in size. In particular, S1B contains 58.7×10^6 parameters, whereas MultiGraspNet-vac. and MultiGraspNet have only 14.6×10^6 and 15.7×10^6 parameters, respectively. This highlights that our approach achieves competitive performance with substantially lower model complexity.

The bottom portion of the table reports the results for parallel grasping. All competing methods in this setting are 3D point-cloud-based and have model capacities comparable to ours. While the single-task variant *MultiGraspNet-par.* achieves slightly lower performance than the best EFG competitor (15.7×10^6 parameters) with a gap of less than one AP point, the full multitask MultiGraspNet attains the best results on both the seen and novel object groups.

Fig. 4 presents qualitative results obtained by MultiGraspNet. Our model successfully generates feasible grasps for both grippers in diverse scenes. We observe that the predicted vacuum poses primarily concentrate on flat and smooth surfaces, such as boxes or planar regions, where vacuum grasping is most effective. In contrast, parallel grasp predictions tend to focus on smaller and more geometrically complex objects. This complementary behavior highlights MultiGraspNet's ability to

TABLE II: Analysis of design variants for MultiGraspNet. Results on the RealSense data of the aligned dual-gripper dataset from SuctionNet-1Billion (Vacuum) and GraspNet-1Billion (Parallel). Top results are in bold, while the second best are underlined.

Model	Parallel										Vacuum									
	Seen			Similar			Novel				Seen			Similar			Novel			
	AP	AP _{0.8}	AP _{0.4}	AP	AP _{0.8}	AP _{0.4}														
MultiGraspNet w/o PCGrad	69.18	80.00	65.13	60.08	72.59	52.33	24.92	30.75	13.41	26.70	2.90	34.60	28.54	2.86	37.02	8.64	0.49	10.56		
MultiGraspNet w RGB	67.09	78.19	62.07	58.49	70.60	50.73	24.10	29.80	12.86	<u>27.22</u>	<u>3.01</u>	<u>35.22</u>	<u>30.06</u>	<u>3.40</u>	<u>39.35</u>	<u>7.57</u>	0.41	<u>9.40</u>		
MultiGraspNet	68.37	79.61	64.02	60.28	<u>72.54</u>	52.87	25.53	31.67	13.66	28.07	3.62	35.81	31.22	3.53	41.65	7.38	<u>0.46</u>	8.92		

adapt to the distinct operational properties of different grippers.

C. Exploring Design Variants

Here, we provide a detailed analysis of how key design choices of MultiGraspNet contribute to its performance. In particular, we examine the role of gradient surgery in multitask training and the impact of incorporating color features to enrich the input scene representation. We empirically show that employing the former and excluding the latter yields overall quantitative advantages across tasks.

1) *Gradient Surgery for Multitask Learning*: multitask learning often suffers from optimization challenges due to gradient interference between tasks, which can lead to imbalanced training and cause certain tasks to dominate the learning process. As mentioned in section III-D, we incorporate the PCGrad [29] technique into our training process. It projects the parallel and vacuum task gradients onto non-interfering subspaces and mitigates the issue of conflicting gradient updates. Here, we compare the performance of MultiGraspNet trained with the Adam optimizer with and without (w/o) PCGrad.

As shown in Table II, the model without PCGrad achieves noticeable improvements in specific data groups and tasks, namely parallel/seen and vacuum/novel, albeit at the cost of decreased performance across other splits. To provide a single summary metric for task performance, we average the AP values across the three categories (seen, similar, and novel) for each gripper, and we name it \overline{AP} . The performance of our model using just the Adam optimizer results in $\overline{AP}_p = 51.39$ for parallel and $\overline{AP}_v = 21.29$ for vacuum. When incorporating PCGrad, MultiGraspNet yields $\overline{AP}_p = 51.39$ for parallel and $\overline{AP}_v = 22.22$ for vacuum. We conclude that PCGrad helps to maintain a competitive performance on the parallel task while also improving on the vacuum task, leading to a more balanced and consistent performance across grasping modalities and splits. Thus, we always train our model with PCGrad.

2) *Adding RGB features*: To test whether additional color information could improve scene understanding, we extend our model to incorporate 2D RGB features extracted from a pretrained ResNet-18 backbone. They are concatenated with the 3D features obtained from the point cloud, allowing the network to leverage both geometric and appearance-based cues. As shown in Table II, MultiGraspNet with (w) RGB features underperforms across tasks and splits with a small advantage only on novel objects for the vacuum gripper. These findings indicate that, within our setup, adding color information does not provide a reliable benefit and may even introduce unnecessary complexity without improving grasping

performance. Thus, we decided not include RGB data for training our model.

D. Small-data Regime

In large-scale data regimes, the advantages of multitask learning can be less pronounced, as task-specific models often have sufficient labeled data to independently learn accurate representations and mappings. In contrast, when only a limited number of labeled scenes is available, the ability to share information across tasks becomes critical for robust generalization. In this section, we evaluate our model under such small-data conditions, which more closely reflect real-world deployment scenarios. We focus on a subsampled training set consisting of one to six scenes, drawn uniformly at random. For each training set size, we repeat the experiments ten times. Fig. 5 reports the boxplots of the differences (Δ) between MultiGraspNet and its single-task versions, MultiGraspNet-vac and MultiGraspNet-par. More precisely, (a) and (c) show results for individual object groups in AP , while (b) and (d) report the difference in the average metric \overline{AP} .

For the parallel task, MultiGraspNet exhibits lower AP_p values across splits than the MultiGraspNet-par version from one to five scenes and a higher value using six scenes, with a gain in $\Delta\overline{AP}_p$ of approximately 0.5, associated mainly to the seen object group. Instead, for the vacuum task, MultiGraspNet obtains positive or competitive AP_v across the three object groups, especially for two, three, five and six scenes, with a gain in $\Delta\overline{AP}_v$ of approximately 0.5-1 point. From these results, we observed that in the small-data regime, there is a positive transfer mainly on the vacuum task.

E. Real-world Experiments

To conduct a comprehensive evaluation of our proposed approach, we perform real-world experiments in an industrial setting. Qualitative video demonstrations of the grasp executions are provided in the supplementary material. All experiments are executed using a 6-DoF industrial robotic arm with a maximum lifting capacity of 3 Kg designed for assembly and manipulation, equipped with a RealSense depth camera for 3D perception, as shown in Fig. 6. The end-effector configuration consists of a parallel gripper and a vacuum gripper, coupled via an automated tool changer that enables their rapid switching during operation.

As a baseline comparison, we first test the reference single-gripper methods independently for each gripper type.

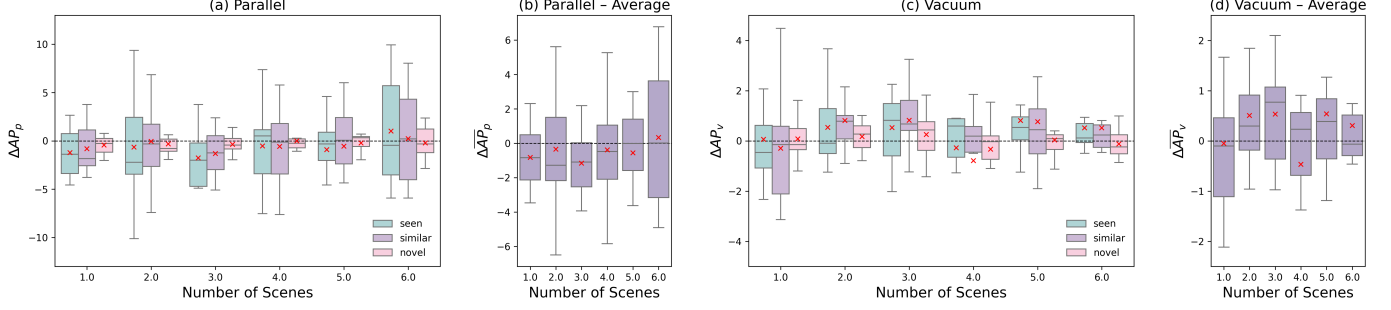


Fig. 5: Small Data Regime: panels (a) and (c) show the performance difference of MultiGraspNet with MultiGraspNet-par and MultiGraspNet-vac over different object groups. The (b) and (d) panels present the average \overline{AP} discrepancy. In each box plot, the red cross indicates the mean, while the horizontal line is the median, calculated over ten repetitions.



Fig. 6: Setup of our multi-gripper system using a depth camera and a tool changer for flexible gripper use. The setup includes two types of end-effectors: a parallel gripper on the left and a vacuum gripper on the right. Each of them is stored in a dedicated station (2). The automated tool changer (1) facilitates quick switching by connecting directly to the gripper and removing it from its storage station.

Specifically, we utilize S1B [13] for vacuum and EFG [2] for parallel-jaw grasping poses. To quantify the performance, we adopt the following metrics:

- R_{object} : ratio of the number of successfully cleared objects to the total number of objects.
- R_{grasp} (success rate): ratio of the number of successful grasps to the total number of grasps.
- R_{mix} : ratio of the number of grasps (over the successfully cleared objects) to the number of successfully cleared objects.
- R_{seen} : ratio of the number of detected objects to the total number of objects in the scene.

They help to understand whether failures are due to the quality of the grasping pose or perceptual limitations. Specifically, R_{object} , R_{grasp} , and R_{mix} assess the predicted grasp effective-

ness. Instead, R_{seen} focuses on perception quality, quantifying how well the model detects objects in the scene. We adopt the first two exactly as defined in [13], while we use the inverse of R_{mix} from the same work to more intuitively reflect the number of attempts required to successfully grasp an object. Finally, we propose R_{seen} , motivated by the observation that models tend to detect some objects more frequently than others.

We adopt the same experimental setup as previous works [2], [12], [20]. For each trial, the system processes the input point cloud and predicts grasp candidates. The one with the highest score is selected and executed. After each attempt, the system re-evaluates the remaining objects in the scene and repeats the process. The cycle continues until all objects are successfully cleared from the table or the robot fails to grasp any object for three consecutive times. To assess performance in diverse cluttered environments, we consider ten test scenes belonging to the following categories:

- *Seen objects*: 20 objects from the G1B [20] objects set are considered. Each scene is populated by randomly arranging six objects from the seen objects in Fig. 6 (bottom). This setup ensures variability in object shape, texture, and physical properties. Five scenes are generated, resulting in 30 total objects, with some objects repeated across scenes.
- *Unseen objects*: 15 completely new objects are considered. Each scene includes five randomly selected objects from a new object set. As shown in Fig. 6 (bottom), the unseen items introduce new shapes, colors, and deformable objects, allowing us to assess the capabilities of our model. Five scenes are created, comprising 25 objects in total.

The results reported in Table III indicate that, for the vacuum task, our approach successfully grasps a larger number of objects than S1B [13], as reflected by the R_{object} metric. This improvement is related to the higher R_{seen} achieved by our model, suggesting more accurate object perception within the scene. Moreover, in terms of R_{grasp} , our approach outperforms S1B, with particularly noticeable gains on unseen objects. In this setting, our model also requires fewer grasp attempts to achieve successful picks, as evidenced by the higher R_{mix} .

For parallel grasping, MultiGraspNet outperforms EFG [2], although the gain is less pronounced. On the seen objects, the value of R_{object} indicates that our method allows to grasp one more object than the competitor, with improved values for

TABLE III: Real Experiments Performance.

Method	vacuum				Unseen			
	Seen	Unseen	Seen	Unseen	Seen	Unseen	Seen	Unseen
S1B [13]	16/30 (53%)	39.11%	1.14	24/30 (80%)	12/25 (48%)	43.33%	1.17	17/25 (68%)
MultiGraspNet	21/30 (70%)	41.02%	1.34	30/30 (100%)	20/25 (80%)	54.76%	1.14	25/25 (100%)
Parallel								
Method	Seen				Unseen			
	<i>R_{object}</i> ↑	<i>R_{grasp}</i> ↑	<i>R_{mix}</i> ↓	<i>R_{seen}</i> ↑	<i>R_{object}</i> ↑	<i>R_{grasp}</i> ↑	<i>R_{mix}</i> ↓	<i>R_{seen}</i> ↑
EFG [2]	28/30 (93%)	66.03%	1.45	30/30 (100%)	22/25 (88%)	76.98%	1.14	24/25 (96%)
MultiGraspNet	29/30 (96%)	76.64%	1.35	29/30 (96%)	23/25 (92%)	70.48%	1.16	25/25 (100%)
Multi-gripper (post-hoc combination)								
Method	Seen				Unseen			
	<i>R_{object}</i> ↑	<i>R_{grasp}</i> ↑	<i>R_{mix}</i> ↓	<i>R_{seen}</i> ↑	<i>R_{object}</i> ↑	<i>R_{grasp}</i> ↑	<i>R_{mix}</i> ↓	<i>R_{seen}</i> ↑
S1B + EFG	28/30 (93%)	74.00%	1.14	30/30	24/25 (96%)	83.00%	1.08	25/25 (100%)
MultiGraspNet	29/30 (96%)	81.00%	1.24	29/30	25/25 (100%)	93.00%	1.08	25/25 (100%)

R_{grasp} and R_{mix} , indicating a reduced number of grasping attempts. In contrast, for unseen objects the gain in R_{object} , comes with a reduction in R_{grasp} and an increase in R_{mix} , showing that to our method requires a higher number of attempts to grasps one more object than the reference baseline. Finally, concerning R_{seen} , both models exhibit similar results, indicating analogous perception abilities.

To provide further insight into approaches capable of handling multiple end-effectors, we evaluate a post-hoc combination of S1B and EFG, as well as the combination of MultiGraspNet’s single-task variants. In both cases, the integration is performed by selecting, for each scene and each object, the gripper that minimizes the number of attempts required for successful grasping. The bottom part of Table III shows the advantage of MultiGraspNet in terms of grasp success rate R_{grasp} over the considered baseline, despite similar results for the other metrics. We remark that the unified network of our multitask approach provides a much more efficient solution than training two separate models. In general, by using both grippers, our model can be exploited to its full potential, preserving perception quality and a low number of failure attempts.

V. CONCLUSION

We present MultiGraspNet, a multitask 3D deep learning model capable of predicting grasp poses for both parallel-jaw and vacuum grippers within a unified framework. By leveraging complementary information between the two grasping modalities, our model generates accurate grasp poses across a variety of cluttered scenes with diverse objects. Extensive experiments demonstrate that our MultiGraspNet consistently outperforms baseline methods in both seen and unseen object scenarios, with particularly strong gains for vacuum grasping and consistent improvements for parallel grasping in a challenging real-world scenario. By integrating multiple grasping modalities in a shared architecture with a multi-gripper robotic setup, MultiGraspNet provides an accurate and versatile solution for real-world robotic grasping, demonstrating the potential of multitask architectures for multi-gripper robotic grasping.

Future work will investigate the integration of a learning-based gripper selection module or the development of a calibration strategy to directly compare grasp scores across grippers, further improving the system’s consistency.

ACKNOWLEDGMENTS

This work was supported by Comau S.p.A. The authors would like to thank Giovanni Di Stefano, Simone Panicucci, Nicola Longo, Luca Di Ruscio, Luca Robbiano, and Simone Peirone for their valuable assistance. This study was carried out within the FAIR - Future Artificial Intelligence Research and received funding from the European Union Next-GenerationEU (PIANO NAZIONALE DI RIPRESA E RESILIENZA (PNRR) – MISSIONE 4 COMPONENTE 2, INVESTIMENTO 1.3 – D.D. 1555 11/10/2022, PE00000013). This manuscript reflects only the authors’ views and opinions, neither the European Union nor the European Commission can be considered responsible for them. We thank the anonymous reviewers and editor for their constructive comments and suggestions.

REFERENCES

- [1] J. Mahler, J. Liang, S. Niyaz, M. Laskey, R. Doan, X. Liu, J. A. Ojea, and K. Goldberg, “Dex-net 2.0: Deep learning to plan robust grasps with synthetic point clouds and analytic grasp metrics,” *RSS*, 2017.
- [2] X.-M. Wu, J.-F. Cai, J.-J. Jiang, D. Zheng, Y.-L. Wei, and W.-S. Zheng, “An economic framework for 6-dof grasp detection,” in *ECCV*, 2024.
- [3] J. Mahler, M. Matl, X. Liu, A. Li, D. Gealy, and K. Goldberg, “Dex-net 3.0: Computing robust vacuum suction grasp targets in point clouds using a new analytic model and deep learning,” in *ICRA*, 2018.
- [4] R. Cao, B. Yang, Y. Li, C.-W. Fu, P.-A. Heng, and Y.-H. Liu, “Uncertainty-aware suction grasping for cluttered scenes,” *IEEE RAL*, vol. 9, no. 6, pp. 4934–4941, 2024.
- [5] D. Ceschini, R. D. Cesare, E. Civitelli, and M. Indri, “Segmentation-based approach for a heuristic grasping procedure in multi-object scenes,” in *ETFA*, 2024.
- [6] A. Zeng, S. Song, K.-T. Yu, E. Donlon, F. R. Hogan, M. Bauza, D. Ma, O. Taylor, M. Liu, E. Romo *et al.*, “Robotic pick-and-place of novel objects in clutter with multi-affordance grasping and cross-domain image matching,” *IJRR*, vol. 41, pp. 690–705, 2022.
- [7] W. Zhu, C. Lu, Q. Zheng, Z. Fang, H. Che, K. Tang, M. Zhu, S. Liu, and Z. Wang, “A soft-rigid hybrid gripper with lateral compliance and dexterous in-hand manipulation,” *IEEE/ASME Transactions on Mechatronics*, vol. 28, no. 1, pp. 104–115, 2022.
- [8] M. Burgess and E. H. Adelson, “Grasp everything (get): 1-dof, 3-fingered gripper with tactile sensing for robust grasping,” *preprint arXiv:2505.09771*, 2025.
- [9] Y. Hu, M. Li, S. Yang, X. Li, S. Liu, and M. Li, “Learning robust grasping strategy through tactile sensing and adaption skill,” in *2024 IEEE ROBIO*, 2024, pp. 1197–1202.
- [10] M. Fujita, Y. Domae, R. Kawanishi, G. A. G. Ricardez, K. Kato, K. Shiratsuchi, R. Haraguchi, R. Araki, H. Fujiyoshi, S. Akizuki *et al.*, “Bin-picking robot using a multi-gripper switching strategy based on object sparseness,” in *CASE*, 2019.
- [11] A. S. Olesen, B. B. Gergaly, E. A. Ryberg, M. R. Thomsen, and D. Chrysostomou, “A collaborative robot cell for random bin-picking based on deep learning policies and a multi-gripper switching strategy,” *Procedia Manufacturing*, vol. 51, pp. 3–10, 2020.
- [12] Q. Shao, J. Hu, W. Wang, Y. Fang, W. Liu, J. Qi, and J. Ma, “Suction grasp region prediction using self-supervised learning for object picking in dense clutter,” in *ICMSR*, 2019.
- [13] H. Cao, H.-S. Fang, W. Liu, and C. Lu, “Suctionnet-1billion: A large-scale benchmark for suction grasping,” *IEEE RAL*, vol. 6, no. 4, pp. 8718–8725, 2021.
- [14] D.-H. Zhai, S. Yu, Y. Guan, and Y. Xia, “Sgnet: Robotic suction grasp detection with multiscale attention,” *IEEE/ASME Transactions on Mechatronics*, vol. 30, no. 6, pp. 6927–6938, 2025.
- [15] C. Xie, Y. Xiang, A. Mousavian, and D. Fox, “Unseen object instance segmentation for robotic environments,” *IEEE TRO*, vol. 37, no. 5, pp. 1343–1359, 2021.
- [16] Y. Jiang, S. Moseon, and A. Saxena, “Efficient grasping from rgbd images: Learning using a new rectangle representation,” in *ICRA*, 2011.
- [17] I. Lenz, H. Lee, and A. Saxena, “Deep learning for detecting robotic grasps,” *IJRR*, vol. 34, no. 4–5, pp. 705–724, 2015.
- [18] U. Asif, J. Tang, and S. Harrer, “Densely supervised grasp detector (dsgd),” in *AAAI*, 2019.

- [19] M. Gou, H.-S. Fang, Z. Zhu, S. Xu, C. Wang, and C. Lu, “Rgb matters: Learning 7-dof grasp poses on monocular rgbd images,” in *ICRA*, 2021.
- [20] H.-S. Fang, C. Wang, M. Gou, and C. Lu, “Graspnet-1billion: A large-scale benchmark for general object grasping,” in *CVPR*, 2020.
- [21] C. Wang, H.-S. Fang, M. Gou, H. Fang, J. Gao, and C. Lu, “Graspness discovery in clutters for fast and accurate grasp detection,” in *ICCV*, 2021.
- [22] A. Alliegro, M. Rudorfer, F. Frattin, A. Leonardis, and T. Tommasi, “End-to-end learning to grasp via sampling from object point clouds,” *IEEE RAL*, vol. 7, no. 4, pp. 9865–9872, 2022.
- [23] H. Ma, M. Shi, B. Gao, and D. Huang, “Generalizing 6-dof grasp detection via domain prior knowledge,” in *CVPR*, 2024.
- [24] D. Morrison, A. W. Tow, M. McTaggart, R. Smith, N. Kelly-Boxall, S. Wade-Mccue, J. Erskine, R. Grinover, A. Gurman, T. Hunn *et al.*, “Cartman: The low-cost cartesian manipulator that won the amazon robotics challenge,” in *ICRA*, 2018.
- [25] J. Mahler, M. Matl, V. Satish, M. Danielczuk, B. DeRose, S. McKinley, and K. Goldberg, “Learning ambidextrous robot grasping policies,” *Science Robotics*, vol. 4, no. 26, pp. 1373–1379, 2019.
- [26] Y. G. Son, S. Um, J. Hong, T. H. Bui, and H. R. Choi, “Corner-grasp: Multi-action grasp detection and active gripper adaptation for grasping in cluttered environments,” *preprint arXiv:2504.01861*, 2025.
- [27] C. Choy, J. Gwak, and S. Savarese, “4d spatio-temporal convnets: Minkowski convolutional neural networks,” in *CVPR*, 2019.
- [28] Q.-Y. Zhou, J. Park, and V. Koltun, “Open3d: A modern library for 3d data processing,” *preprint arXiv:1801.09847*, 2018.
- [29] T. Yu, S. Kumar, A. Gupta, S. Levine, K. Hausman, and C. Finn, “Gradient surgery for multi-task learning,” *NeurIPS*, 2020.